Noise-Like Structure in the Image of Diffusely Reflecting Objects in Coherent Illumination

By L. H. ENLOE

(Manuscript received April 13, 1967)

Holographic and other imaging systems utilizing coherent light introduce a speckled or noise-like pattern in the image of a diffuse object which severely degrades image quality. It is desirable to understand this effect quantitatively. Intelligent design in many cases requires knowledge of the mean-square value, spatial power spectral density, and autocorrelation function of the noise-like fluctuations. These quantities have been determined for the image of a uniform diffuse object. Major results are:

(i) The mean-square value of the fluctuation in the image intensity is equal to the square of the mean intensity.

(ii) One can decrease the relative magnitude of the noise-like fluctuations at the cost of a corresponding increase in the aperture required of the optical system (or hologram) over that required to resolve the desired image in a spatial frequency sense. In a holographic facsimile or TV system, this calls for a corresponding increase in electrical bandwidth.

(iii) The improvement in (ii) is not possible for direct viewing with the human eye, since the resolution of a healthy eye is known to be limited by diffraction at the iris.

I. INTRODUCTION

Holographic and other imaging systems using coherent light have been receiving considerable attention lately.[1,2,3,4] Most analyses on this subject assume that the object reflects specularly, or transmits specularly if the object is a transparency, i.e., the reflectivity or transmissivity of the object varies smoothly. Most objects, however, are more nearly diffuse reflectors. When the image of a diffusely reflecting object is formed it will be covered with a noise or grain-like structure[5,6,7] which is the speckle pattern which one sees when laser light is used to illuminate an object.

In this paper we investigate the noise-like or speckled nature of the image of a uniform diffuse surface. It should be emphasized that we are interested in the properties of the image in contradistinction to the direct backscattered field studied by Goldfisher.[8] We show that the intensity consists of two parts. The first is the mean or ensemble average intensity and is proportional to the intensity which would be obtained if incoherent light were used for illumination. This is the desired component of the image and might be likened to a signal. The second part of the image is the speckled or noise-like component which tends to obscure the average intensity. This noise-like component occurs because of the random phase angles associated with the scattering centers comprising the microstructure of the diffuse surface. The spatial autocorrelation function and power spectral density of the speckle pattern in the image are found, and are shown to be dependent upon the size of the aperture stop. It is shown that the variance of the intensity fluctuation is equal to the square of the mean intensity. The fluctuation may be reduced, however, if one is willing to sacrifice resolution by recording the image on film whose resolution is much poorer than that set by the aperture of the optics. Unfortunately, this alternative is not available when viewing with the human eye, since the resolution of a healthy eye is known to be determined by the diffraction limit of the iris.[9] This seems to place definite limitations upon the use of coherent light in visual systems.

II. ARBITRARY APERTURE

The model which we shall use for a diffuse object is shown in Fig. 1. Although the object is shown to be a granular transparency, it could equally well have been shown as a reflector without loss of generality. The essential point is that a monochromatic coherent light wave of unit intensity is assumed to be scattered by a random set of point scatterers. Each scatterer is assumed to be a unit scatterer which is many wavelengths in depth from its neighbor. The relative phase of the wave scattered from each scatterer may be assumed to be a random variable which is statistically independent of the phase of the waves scattered from other scatterers. Any phase change between 0 and 2π is equally likely. Multiple scattering will be neglected.

The scattered field just to the right of the granular transparency can be expressed by the equation

$$F_0(x, y) = \sum_{i=1}^{K} \delta(x - x_i , y - y_i)\epsilon^{i\theta_i}, \tag{1}$$

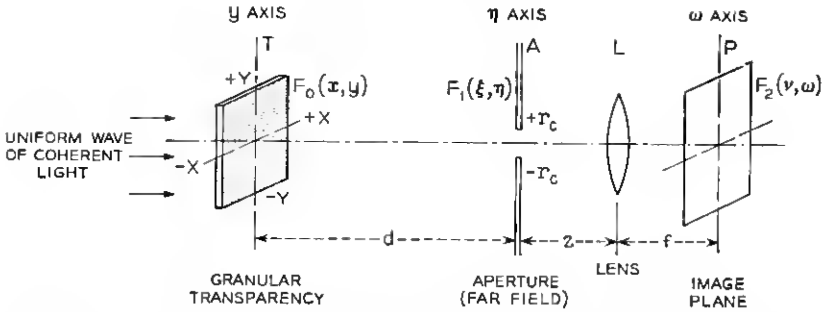

Fig. 1 — A uniform wave of coherent light is incident on a transparency composed of randomly distributed unit point scatterers. Light collected by the aperture A, placed in the far-field, is imaged by lens L on plane P.

where θ_i is the relative phase of the wave scattered from the scatterer located at $x = x_i$, $y = y_i$. θ_i, x_i and y_i are assumed to be random variables uniformly distributed in the intervals $(0,2\pi)$, $(-X,+X)$ and $(-Y,+Y)$, respectively. Notice that because of our assumptions, the statistics of the scattered field are independent of any deterministic variation in the phase of the illuminating field.

A Fourier transform relationship exists between the scattered field given by (1) and its far-field. The far-field is given by

$$\begin{aligned} F_1(\xi, \eta) &= \int_{-\infty}^{+\infty} \int_{-\infty}^{+\infty} F_0(x, y)\epsilon^{j(2\pi/\lambda d)(x\xi+y\eta)}\, dx\, dy \\ &= \sum_{i=1}^{K} \epsilon^{j\theta_i + j(2\pi/\lambda d)(x_i\xi+y_i\eta)}, \end{aligned} \tag{2}$$

where we have suppressed the time factor $\epsilon^{+j\Omega t}$. Notice that each scatterer has produced a plane wave, and that the slope of the phase front of each wave with respect to the ξ, η axes is determined by the position (x_i, y_i) of the random scatterer.

Let the far-field $F_1(\xi, \eta)$ be passed through an aperture having an amplitude transmission function $H(\xi, \eta)$, and then through a lens which is placed a distance z behind the aperture. Since the field at the back focal plane of a lens is a Fourier transform like function of the field in front of the lens, an image of the granular transparency, as modified by the aperture, will be formed in the back focal plane, and is given by[10]

$$\begin{aligned} F_2(\nu, \omega) &= \epsilon^{jc(\nu^2+\omega^2)} \int_{-\infty}^{+\infty} \int_{-\infty}^{+\infty} H(\xi, \eta)F_1(\xi, \eta)\epsilon^{j(2\pi/\lambda f)(\xi\nu+\eta\omega)}\, d\xi\, d\eta \\ &= \epsilon^{jc(\nu^2+\omega^2)} \sum_{i=1}^{K} h\left(\frac{\nu}{\lambda f} + \frac{x_i}{\lambda d}, \frac{\omega}{\lambda f} + \frac{y_i}{\lambda d}\right)\epsilon^{j\theta_i}, \end{aligned} \tag{3a}$$

where $c = \pi(z - f)/\lambda f^2$, and where $h(t, u)$ and $H(\xi, \eta)$ are Fourier transform pairs in the sense

$$h(t, u) = \int_{-\infty}^{+\infty} \int_{-\infty}^{+\infty} H(\xi, \eta)\epsilon^{j2\pi(\xi t + \eta u)} \, d\xi \, d\eta. \tag{3b}$$

Notice that except for the unimportant phase factor $\epsilon^{jc(\nu^2+\omega^2)}$, (3a) differs from (1) for the field at the granular transparency only in that $h(\ )$ functions have replaced the delta functions. That is to say, the delta function of light from the scatterer at (x_i, y_i) is reproduced as a broadened $h(\ )$ function located at $\nu = -(f/d)x_i$, $\omega = -(f/d)y_i$. The image is reversed, and magnified by the factor $m = f/d$. Notice that because of the random phase θ_i of each, the impulse functions will add vectorially in a random fashion when they overlap one another.

The situation is analogous to passing shot noise impulses through a low-pass filter having an impulse response $h(\ )$. The impulses are broadened into $h(\ )$ pulses whose width depends inversely upon the filter bandwidth. In the coherent light case, however, the process is two dimensional and the applied impulses have random phase angles distributed uniformly between 0 and 2π, rather than being constrained to be positive impulse functions as is the case for shot noise.

The quantity of greatest interest to us is the intensity of the image, which is found by multiplying the image field by its conjugate.

$$\begin{aligned} I(\nu, \omega) &= F_2(\nu, \omega)F_2^*(\nu, \omega) \\ &= \sum_{k=1}^{K} \sum_{i=1}^{K} h\left(\frac{\nu}{\lambda f} + \frac{x_k}{\lambda d}, \frac{\omega}{\lambda f} + \frac{y_k}{\lambda d}\right) \cdot h^*\left(\frac{\nu}{\lambda f} + \frac{x_i}{\lambda d}, \frac{\omega}{\lambda f} + \frac{y_i}{\lambda d}\right) \epsilon^{j(\theta_k - \theta_i)}. \end{aligned} \tag{4}$$

The uniform diffuse object is assumed to exist in the region $-X \leqq x \leqq +X$, $-Y \leqq y \leqq +Y$. The number K of point scatterers in this region is a random variable, as are their positions (x_i, y_i) and their relative phase angles θ_i. We may, therefore, obtain the ensemble average of the image intensity I by averaging (4) with respect to the $2K + 1$ random variables consisting of the K positions (x_i, y_i), K phase angles θ_i, and K itself:

$$\begin{aligned} \bar{I} = \int_{-\infty}^{+\infty} \cdots \int_{-\infty}^{+\infty} &\left[\sum_{k=1}^{K} h\left(\frac{\nu}{\lambda f} + \frac{x_k}{\lambda d}, \frac{\omega}{\lambda f} + \frac{y_k}{\lambda d}\right) \epsilon^{j\theta_k} \right] \\ &\cdot \left[\sum_{i=1}^{K} h^*\left(\frac{\nu}{\lambda f} + \frac{x_i}{\lambda d}, \frac{\omega}{\lambda f} + \frac{y_i}{\lambda d}\right) \epsilon^{-j\theta_i} \right] \\ &\cdot W(x_1, y_1; x_2, y_2; \cdots x_K, y_K; \theta_1; \cdots \theta_K; K) \\ &\cdot dx_1 \, dy_1 \cdots dx_K \, dy_K \, d\theta_1; \cdots d\theta_K \, dK, \end{aligned} \tag{5}$$

where $W(\ )$ is the multi-dimensional probability density function.

Now the positions (x_l, y_l) are considered to be statistically independent variables, as are the relative phase angles θ_l. They are also independent of K, so we may simplify (5) to obtain

$$\bar{I} = \int_{-\infty}^{+\infty} W(K)\,dK \cdot \left[\sum_{k=1}^{K}\sum_{i=1}^{K}\int_{-X}^{+X}\frac{dx_1}{2X}\cdots\int_{-X}^{+X}\frac{dx_K}{2X}\int_{-Y}^{+Y}\frac{dy_K}{2Y}\int_0^{2\pi}\frac{d\theta_1}{2\pi}\cdots\int_0^{2\pi}\frac{d\theta_K}{2\pi} \cdot\left\{\epsilon^{j(\theta_k-\theta_i)} h\left(\frac{\nu}{\lambda f}+\frac{x_k}{\lambda d}, \frac{\omega}{\lambda f}+\frac{y_k}{\lambda d}\right)\cdot h^*\left(\frac{\nu}{\lambda f}+\frac{x_i}{\lambda d}, \frac{\omega}{\lambda f}+\frac{y_i}{\lambda d}\right)\right\}\right]. \tag{6}$$

We see that the above expression vanishes unless $\theta_i = \theta_k$, i.e., $i = k$. Further, all of the $h(\ )$ functions have the same shape so that if the size of a resolution element in the image is small compared to the field of view, i.e., the extent of $h(\nu/\lambda f, \omega/\lambda f)$ is small compared to X and Y, then we may replace the limits of integration $\pm X$ and $\pm Y$ by $\pm\infty$ to obtain

$$\bar{I} = \frac{d^2\lambda^2\rho_1(0, 0)}{4XY}\int_{-\infty}^{+\infty} KW(K)\,dK. \tag{7}$$

$\rho_1(u, v)$ is the autocorrelation function of the aperture impulse function $h(\xi, \eta)$, i.e.,

$$\begin{aligned}\rho_1(u, v) &= \int_{-\infty}^{+\infty}\int_{-\infty}^{+\infty} h^*(t, \tau)h(t+u, \tau+v)\,dt\,d\tau \\ &= \int_{-\infty}^{+\infty}\int_{-\infty}^{+\infty} H(\xi, \eta)H^*(\xi, \eta)\epsilon^{j2\pi(\xi u+\eta v)}\,d\xi\,d\eta.\end{aligned} \tag{8}$$

If we now assume that the number of scatterers per unit area of the transparency has a Poisson distribution of mean $\bar{N}$, then the mean intensity is

$$\bar{I} = d^2\lambda^2\bar{N}\rho_1(0, 0). \tag{9}$$

Next we wish to determine an expression for the autocorrelation function of the intensity, from which we may determine the spatial power spectral density and variance of the noise-like fluctuations. The autocorrelation function of the intensity as given by (4) is

$$\begin{aligned}R(\tau, t) &= \overline{I_2(\nu, \omega)I_2(\nu+\tau, \omega+t)} \\ &= \int_{-\infty}^{+\infty}\cdots\int_{-\infty}^{+\infty}\left[\sum_{k=1}^{K} h\left(\frac{\nu}{\lambda f}+\frac{x_k}{\lambda d}, \frac{\omega}{\lambda f}+\frac{y_k}{\lambda d}\right)\epsilon^{j\theta_k}\right]\end{aligned} \tag{10}$$

$$\cdot\left[\sum_{i=1}^{K} h^*\left(\frac{\nu}{\lambda f}+\frac{x_i}{\lambda d}, \frac{\omega}{\lambda f}+\frac{y_i}{\lambda d}\right)\epsilon^{-j\theta_i}\right]$$
$$\cdot\left[\sum_{m=1}^{K} h\left(\frac{\nu+\tau}{\lambda f}+\frac{x_m}{\lambda d}, \frac{\omega+t}{\lambda f}+\frac{y_m}{\lambda d}\right)\epsilon^{j\theta_m}\right]$$
$$\cdot\left[\sum_{n=1}^{K} h^*\left(\frac{\nu+\tau}{\lambda f}+\frac{x_n}{\lambda d}, \frac{\omega+t}{\lambda f}+\frac{y_n}{\lambda d}\right)\epsilon^{-j\theta_n}\right]$$
$$\cdot W(x_1\,,\, y_1\,;\, x_2\,,\, y_2\,;\, \cdots\, x_K y_K\,;\, \theta_1\,;\, \cdots\, \theta_K\,,\, K)\, dx_1 \cdots dK.$$

Because of the statistical independence of the phase angles θ_i, positions (x_i, y_i) and K, and because of the assumed uniform distribution, we may simplify (10) to

$$R(\tau, t) = \int_{-\infty}^{+\infty} W(K)\, dK$$
$$\cdot \sum_{k=1}^{K}\sum_{i=1}^{K}\sum_{m=1}^{K}\sum_{n=1}^{K}\int_{-\infty}^{+\infty}\frac{dx_1}{2X}\int_{-\infty}^{+\infty}\frac{dy_1}{2Y}\cdots\int_{-\infty}^{+\infty}\frac{dx_K}{2X}\int_{-\infty}^{+\infty}\frac{dy_K}{2Y}$$
$$\cdot\int_0^{2\pi}\frac{d\theta_1}{2\pi}\cdots\int_0^{2\pi}\frac{d\theta_K}{2\pi}\left[\epsilon^{j(\theta_k-\theta_i+\theta_m-\theta_n)}h\left(\frac{\nu}{\lambda f}+\frac{x_k}{\lambda d}, \frac{\omega}{\lambda f}+\frac{y_k}{\lambda d}\right)\right.$$
$$\cdot h^*\left(\frac{\nu}{\lambda f}+\frac{x_i}{\lambda d}, \frac{\omega}{\lambda f}+\frac{y_i}{\lambda d}\right)h\left(\frac{\nu+\tau}{\lambda f}+\frac{x_m}{\lambda d}, \frac{\omega+t}{\lambda f}+\frac{y_m}{\lambda d}\right)$$
$$\left.\cdot h^*\left(\frac{\nu+\tau}{\lambda f}+\frac{x_n}{\lambda d}, \frac{\omega+t}{\lambda f}+\frac{y_n}{\lambda d}\right)\right]. \tag{11}$$

We see that the integral vanishes unless

$$i = k \qquad \text{and} \qquad n = m$$

or

$$n = k \qquad \text{and} \qquad i = m,$$

which gives

$$R(\tau, t) = \int_{-\infty}^{+\infty} W(K)\, dK$$
$$\cdot \sum_{k=1}^{K}\sum_{m=1}^{K}\int_{-\infty}^{+\infty}\frac{dx_1}{2X}\int_{-\infty}^{+\infty}\frac{dy_1}{2Y}\cdots\int_{-\infty}^{+\infty}\frac{dx_K}{2X}\int_{-\infty}^{+\infty}\frac{dy_K}{2Y}$$
$$\cdot\left|h\left(\frac{\nu}{\lambda f}+\frac{x_k}{\lambda d}, \frac{\omega}{\lambda f}+\frac{y_k}{\lambda d}\right)\right|^2\left|h\left(\frac{u+\tau}{\lambda f}+\frac{x_m}{\lambda d}, \frac{\omega+t}{\lambda f}+\frac{y_m}{\lambda d}\right)\right|^2$$
$$+ h\left(\frac{\nu}{\lambda f}+\frac{x_k}{\lambda d}, \frac{\omega}{\lambda f}+\frac{y_k}{\lambda d}\right)\cdot h^*\left(\frac{\nu+\tau}{\lambda f}+\frac{x_k}{\lambda d}, \frac{\omega+t}{\lambda f}+\frac{y_k}{\lambda d}\right)$$
$$\cdot h^*\left(\frac{\nu}{\lambda f}+\frac{x_m}{\lambda d}, \frac{\omega}{\lambda f}+\frac{y_m}{\lambda d}\right)h\left(\frac{\nu+\tau}{\lambda f}+\frac{x_m}{\lambda d}, \frac{\omega+t}{\lambda f}+\frac{y_m}{\lambda d}\right). \tag{12}$$

Now, we have two subcases here. There are $K(K-1)$ terms for which $k \neq m$, and there are K terms for which $k = m$.

$$R(\tau, t) = \int_{-\infty}^{+\infty} K(K-1)W(K)\, dK$$
$$\cdot\left\{\left[\frac{1}{4XY}\int_{-\infty}^{+\infty}\int_{-\infty}^{+\infty}\left| h\left(\frac{\nu}{\lambda f}+\frac{x}{\lambda d}, \frac{\omega}{\lambda f}+\frac{y}{\lambda d}\right)\right|^2 dx\, dy\right]\right.$$
$$+\left|\frac{1}{4XY}\int_{-\infty}^{+\infty}\int_{-\infty}^{+\infty} h^*\left(\frac{\nu}{\lambda f}+\frac{x}{\lambda d}, \frac{\omega}{\lambda f}+\frac{y}{\lambda d}\right)\right.$$
$$\left.\left.\cdot h\left(\frac{\nu+\tau}{\lambda f}+\frac{x}{\lambda d}, \frac{\omega+t}{\lambda f}+\frac{y}{\lambda d}\right) dy\, dx\right|^2\right\}$$
$$+ 2\int_{-\infty}^{+\infty} KW(K)\, dK$$
$$\cdot\left[\frac{1}{4XY}\int_{-\infty}^{+\infty}\int_{-\infty}^{+\infty}\left| h\left(\frac{\nu}{\lambda f}+\frac{x}{\lambda d}, \frac{\omega}{\lambda f}+\frac{y}{\lambda d}\right)\right|^2\right.$$
$$\left.\cdot\left| h\left(\frac{\nu+\tau}{\lambda f}+\frac{x}{\lambda d}, \frac{\omega+t}{\lambda f}+\frac{y}{\lambda d}\right)\right|^2 dy\, dx\right]. \quad (13)$$

Assuming that the distribution of scatterers $W(K)$ is Poisson and using the definition of h ( ) given in (3b), straightforward evaluation of the integrals in (13) yields

$$R(\tau, t) = \bar{I}^2\left[1 + \frac{|\rho_1(\tau/f\lambda, t/f\lambda)|^2}{\rho_1(0, 0)^2}\right] + 2\frac{\bar{I}}{\rho_1(0, 0)}\rho_2(\tau/f\lambda, t/f\lambda), \quad (14)$$

where ρ_1 (u, v) is defined in (8) and

$$\rho_2(u, v) = \int_{-\infty}^{+\infty}\int_{-\infty}^{+\infty} |h(\tau, t)|^2\, |h(\tau+u, t+v)|^2\, d\tau\, dt$$

= autocorrelation function of the magnitude squared of the aperture impulse function.

The spatial power spectral density is found by taking the Fourier transform of (14). After simplification we obtain

$$S(q, p) = \int_{-\infty}^{+\infty}\int_{-\infty}^{+\infty} R(\tau, t)\epsilon^{-j2\pi(\tau q + tp)}\, d\tau\, dt$$
$$= \bar{I}^2\left\{\delta(q, p) + \frac{(f\lambda)^2}{\rho_1(0, 0)^2}\,|H(\lambda fq, \lambda fp)|^2 \circledast |H(\lambda fq, \lambda fp)|^2\right.$$
$$\left. + \frac{2(f\lambda)^2}{\rho_1(0, 0)\bar{I}}\,|H(\lambda fq, \lambda fp) \circledast H(\lambda fq, \lambda fp)|^2\right\}, \quad (15)$$

where $\circledast$ stands for convolution. In particular we define

$$F(\lambda fq, \lambda fp) \circledast G(\lambda fq, \lambda fp) = \int_{-\infty}^{+\infty} \int_{-\infty}^{+\infty} F^*(x, y) G(\lambda fq + x, \lambda fp + y)\, dy\, dx. \tag{16}$$

Equation (9), which gives the mean intensity of the image, and (15), which gives the power spectral density of the intensity fluctuations, are the major results of this section.

III. CIRCULAR APERTURE

Now consider the special case of a circular aperture of radius r_c, and let it be located on axis so that

$$H(\xi, \eta) = \begin{cases} 1, & r \leqq r_c\,, \\ 0 & r > r_c\,, \end{cases} \tag{17}$$

where

$$r = +\sqrt{\xi^2 + \eta^2}.$$

The average intensity in the image plane is given by (9) and is

$$\bar{I} = d^2\lambda^2\bar{N}\rho_1(0, 0) = \pi\bar{N}(\lambda d r_c)^2, \tag{18}$$

where $\rho_1(0,0)$ was evaluated from the integral

$$\rho_1(0, 0) = \int_{-\infty}^{+\infty} \int_{-\infty}^{+\infty} |H(\xi, \eta)|^2\, d\xi\, d\eta = \pi r_c^2\,. \tag{19}$$

Evaluation of the integrals in (15) gives the power spectral density

$$S(q, p) = \bar{I}^2 \Bigg[\delta(q, p) + \frac{1}{\pi s_c^2} \Bigg\{ 1 - \frac{2}{\pi} \sin^{-1}\left(\frac{s}{2s_c}\right) - \frac{2}{\pi}\left(\frac{s}{2s_c}\right)\sqrt{1 - \left(\frac{s}{2s_c}\right)^2} + \frac{1}{F}\left(1 - \frac{2}{\pi}\sin^{-1}\left(\frac{s}{2s_c}\right) - \frac{2}{\pi}\left(\frac{s}{2s_c}\right)\sqrt{1 - \left(\frac{s}{2s_c}\right)^2}\right)\Bigg\}\Bigg], \tag{20}$$

where

q, p = image plane spatial frequencies in rectangular coordinates,

$s = +\sqrt{q^2 + p^2}$

$s_c = r_c/f\lambda$ = cutoff frequency produced by diffraction at the circular aperture.

$$F = \frac{d^2\lambda^2\bar{N}}{2\pi r_c^2}$$

= overlap factor.

The overlap factor F warrants some discussion. Basically it is equal to the average number of point scatterer image centers contained within an area equal to that occupied by the image of a single scatterer. That is, a single point scatterer located at (0,0) in the object plane would produce a point in the image plane at (0,0) having intensity

$$I = \left| h\left(\frac{\nu}{\lambda f}, \frac{\omega}{\lambda f}\right) \right|^2$$

$$= I_0 \left[\frac{2J_1\left(\frac{2\pi r_c}{f\lambda} \sqrt{\nu^2 + \omega^2}\right)}{\frac{2\pi r_c}{f\lambda} \sqrt{\nu^2 + \omega^2}} \right]^2 .$$

The intensity is down[11] approximately 50 percent at $(2\pi r_c/f\lambda) \sqrt{\nu_1^2 + \omega_1^2} = \sqrt{2}$, and the area covered by the image of the point scatterer at this 50 percent value is $A = \pi(\nu_1^2 + \omega_1^2) = f^2\lambda^2/2\pi r_c^2$. For a diffuse object, the average number of imaged scattering centers per unit area in the image plane is $\bar{n} = (d/f)^2\bar{N}$. If we define the overlap factor F as the average number of scatterer image centers falling in the area of one of these images we have

$$F = \bar{n}A = \frac{d^2\lambda^2\bar{N}}{2\pi r_c^2}.$$

For a truly diffuse surface, the overlap factor $F \gg 1$ so that (20) reduces to

$$S(q, p) = \bar{I}^2 \left[\delta(q, p) + \frac{1}{\pi s_c^2} \left\{ 1 - \frac{2}{\pi} \sin^{-1}\left(\frac{s}{2s_c}\right) - \frac{2}{\pi}\left(\frac{s}{2s_c}\right)\sqrt{1 - \left(\frac{s}{2s_c}\right)^2} \right\} \right] \tag{21}$$

which is plotted in Fig. 2. Note that it is symmetrical about the vertical axis. For very small spatial frequencies, (21) can be approximated by

$$S(q, p) = \bar{I}^2 \left[\delta(q, p) + \frac{1}{\pi s_c^2} \right]. \tag{22}$$

The total fluctuation or noise power occurring in spatial frequencies less than some frequency s_1 is

$$P = \bar{I}^2 \left(\frac{1}{\pi s_c^2} \right)(\pi s_1^2) = \bar{I}^2 \left(\frac{s_1}{s_c} \right)^2. \tag{23}$$

IV. CONCLUSIONS

We have found that the image of a uniform diffuse object illuminated with monochromatic coherent light consists of two parts. The first is the mean or ensemble average given by (18), for a circular aperture, and is proportional to the intensity which would be obtained if noncoherent light were used for illumination. This is the desired component and might be likened to the signal component of the image. The square of this term appears as the first term in (20), (21), and (22), and as the delta function in Fig. 2. The second part of the image is a grainy or noise-like component which tends to obscure the mean intensity or signal. This noise-like component occurs because of the random phase angles associated with the point scatterers comprising the microstructure of the diffuse object. This component is shown as the second term in (20), (21), and (22), and as the continuous part of the power spectrum in Fig. 2. Integration of (21) shows that the variance of the noise-like fluctuations in the intensity is equal to the square of the mean intensity (or to the signal power). This is fortunate to the extent that when the signal is small, the noise is likewise small. However, while our analysis was for the particular case of a uniform diffuse surface, we can safely predict that for nonuniform diffuse objects fine detail in the image will be largely obscured by the noise-like fluctuations if resolution is limited by diffraction.

The noise-like fluctuations in the image can be reduced if one *records* the image on film whose modulation transfer function has a bandwidth which is much smaller than the diffraction limit of the optical system. The high-frequency noise in Fig. 2 will not be resolved in this case. For instance, if one requires the "signal-to-noise" ratio to be increased from unity to 10^3 (30 dB), then from (23) we see that

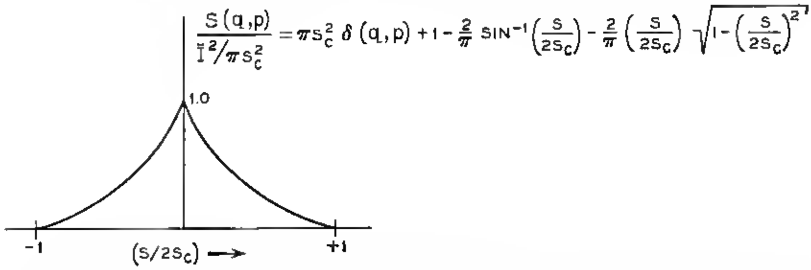

Fig. 2 — Section of the spatial power spectral density for a uniform diffuse surface imaged through a circular aperture. The complete two dimensional spectrum is obtained by rotating the above curve about the vertical axis.

the diffraction bandwidth s_a of the improved optical system must be $10^{3/2} = 31.6$ times the bandwidth s_l resolvable by the film, and therefore by the whole system. (Since most transducers produce a signal which is proportional to the intensity of the incident light, it seems appropriate to consider the square of the mean intensity as signal power and the variance of the intensity fluctuations as noise power.)

Although we have analyzed the very special optical system shown in Fig. 1, our results are not critically dependent upon the placement of the aperture. The aperture could be the lens aperture rather than an independent physical device, or it could be the aperture defined by the finite size of a hologram, for instance. Our results should also hold approximately for the human eye, since the resolution of a healthy eye is known to be determined by the diffraction limit of the iris.[9] The predicted value of unity for the signal-to-noise ratio is the right order of magnitude for what one observes when laser light is used for illumination if one is careful to hold the eye stationary and hence not average the noise out as a function of time. Although moving the eye tends to average out the noise, the residual noisiness remains objectionable. This places definite limitations upon the use of coherent light in visual systems.

The author wishes to thank Messrs. C. B. Rubinstein and A. B. Larsen for helpful discussions.

REFERENCES

1. Cutrona, L. J., Leith, E. N., Palermo, C. J., and Porcello, L. J., Optical Data Processing and Filtering Systems, IRE Trans. Inform. Theory, June, 1960, pp. 386–400.
2. Leith, E. N. and Uptatieks, J., Reconstructed Wavefronts and Communication Theory, J. Opt. Soc. Amer. *52*, No. 10, October, 1962, pp. 1123–1130.
3. Stroke, G. W. and Falconer, D. G., Lensless Fourier-Transform Method for Optical Holography, Appl. Phys. Lett, *6*, No. 10, May 15, 1965, pp. 201–203.
4. Gabor, D., Microscopy by Reconstructed Wavefronts, Proc. Roy. Soc., *A197*, 1949, pp. 454–487.
5. Considine, P. S., Effects of Coherence on Imaging Systems, J. Opt. Soc. Amer. *56*, No. 8, August, 1966, pp. 1001–1008.
6. Rigden, J. D. and Gordon, E. I., The Granularity of Scattered Optical Maser Light, Proc. IRE, *50*, No. 11, November, 1962, pp. 2367–2368.
7. Cutler, C. C., Coherent Light, Int. Sci. Tech., September, 1963, pp. 54–63.
8. Goldfisher, L. I., Autocorrelation Function and Power Spectral Density of Laser-Produced Speckle Patterns, J. Opt. Soc. Amer. *55*, No. 3, March, 1965, pp. 247–253.
9. Graham, C. H. (Editor), *Vision and Visual Perception*, John Wiley and Sons, Inc., New York, 1965, Chapter 11, pp. 321–345.
10. Leith, E. N. and Palermo, C. J., *Introduction to Optical Data Processing*, University of Michigan Engineering Summer Conferences, May 24-June 4, 1965, pp. 2–12 to 2–20.
11. Born, M. and Wolf, E., *Principles of Optics*, Pergamon Press, New York, 1959, p. 396.